Polymer Chemistry

COMMUNICATION

View Article Online
View Journal | View Issue

CrossMark click for updates

Cite this: *Polym. Chem.*, 2016, **7**, 780

Received 11th November 2015,
Accepted 8th December 2015

DOI: 10.1039/c5py01791b

www.rsc.org/polymers

Efficient synthesis and photovoltaic properties of highly rigid perylene-embedded benzothiazolyls†

Runfeng Chen,*[a] Chunhua Zheng,[a] Cong Li,[b] Huanhuan Li,[a] Zhixiang Wang,[a] Yuting Tang,[a] Hongji Jiang,[a] Zhanao Tan*[b] and Wei Huang*[a,c]

Perylene-embedded benzothiazolyls, designed by 2D-fusing of dithienylbenzothiadiazoles (DTBT), have been synthesized and characterized for organic photovoltaic (OPV) applications. A new polymer based on the newly-developed electron-accepting building block exhibits excellent solubility, stability, and photoabsorbability with optimal bandgaps and frontier orbitals, achieving a power efficiency up to 3.22%.

Fuelled by continuous demands on clean, renewable and environmentally friendly energy sources,[1] the rapid development of organic solar cells (OSCs) has been witnessed to show steadily improved organic photovoltaic (OPV) performance with power conversion efficiencies (PCEs) above 9% for single-junction cells[2] and 11% for tandem OSC devices[3] in recent years. The design and synthesis of organic donor materials, which play an indispensable role in effectively harvesting solar energy and transporting dissociated holes mainly in a donor–acceptor (D–A) molecular architecture, is the main engine that powers the dramatic PCE improvements of OSCs.[4] However, in sharp contrast to the high structure versatility of electron-donating building blocks for OPV donor construction, electron-accepting units[5] are limited to several extensively used ones, owing to the intrinsic electron-rich nature of π-conjugated organic aromatic molecules.[6]

4,7-Dithien-2-yl-2,1,3-benzothiadiazole (**DTBT**), as a famous strong acceptor for constructing D–A type OPV molecules, is among the most intensively investigated building blocks for high performance OSCs.[7] Impressively, chemical modifications of **DTBT**, such as fluorine substitution, pyridine replacement and heteroatom bridging, are highly effective in producing new electron-deficient **DTBT** derivatives for OPV materials with a PCE up to 7.2%.[8] Inspired by the 2D collinearly fused molecular structures of polycyclic aromatic hydrocarbons with flat and rigid aromatic π-conjugation and dense molecular packing to tailor not only the single-molecular electronic properties[9] but also the solid-state aggregation and intermolecular interactions[10] with enhanced charge mobility, we reasoned that the forced planarization of **DTBT** by covalently fastening the adjacent thiophene and the central benzothiadiazole may provide a new way to control the bandgap and to enhance the intrinsic charge mobility for high performance OSCs.

The 2D collinearly fused **DTBT** was designed by covalently fusing with ethylene to form a rigid **DTBT** (r-**DTBT**), followed by 2D-fusing with biphenyl to embed a 2D-conjugated perylene structure (Fig. 1), which is flat and highly aromatic for molecular packing control and electronic property adjustment in both the single molecular and aggregated solid states.[11] To increase the solubility and processability, long alkoxy substituents were introduced to afford the target unit (**TNTPT**); **TNTPT** was then copolymerized with a widely used electron-rich benzo[1,2-*b*:4,5-*b*′]dithiophene (BDTT)[12] to test the photovoltaic performance of the newly-developed electron-deficient building block.

The synthesis of 2D-fused perylene-embedded benzothiazolyls commenced with bromination and boronation of benzothiadiazole, iodination of 3-bromothiophene, and alkylation and boronation of 4-bromophenol to prepare **1**, **2**, and **4**,

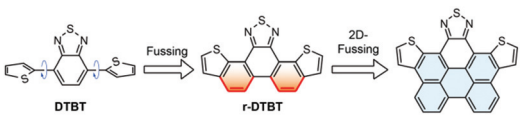

Fig. 1 Molecular design of perylene-embedded benzothiazolyls for OPV applications *via* the 2D-fusing strategy.

[a]*Key Laboratory for Organic Electronics and Information Displays & Institute of Advanced Materials, Jiangsu National Synergistic Innovation Center for Advanced Materials, Nanjing University of Posts & Telecommunications, 9 Wenyuan Road, Nanjing 210023, China. E-mail: iamrfchen@njupt.edu.cn*
[b]*Beijing Key Laboratory of Novel Thin Film Solar Cells, North China Electric Power University, Beijing 102206, China. E-mail: tanzhanao@ncepu.edu.cn*
[c]*Key Laboratory of Flexible Electronics & Institute of Advanced Materials (IAM), Jiangsu National Synergistic Innovation Center for Advanced Materials, Nanjing Tech University (Nanjing Tech), 30 South Puzhu Road, Nanjing 211816, China. E-mail: wei-huang@njtech.edu.cn*

†Electronic supplementary information (ESI) available: Synthetic procedures and characterization data for all compounds, cyclic voltammograms, DFT calculations, device fabrication and measurements. See DOI: 10.1039/c5py01791b

respectively.[13] The Suzuki coupling reaction between **1** and **2** produces **3**, which subsequently reacts with **4** to give **5** also *via* Suzuki cross-coupling catalysed by a palladium(0) complex in good yields (see synthesis and characterization in the ESI, Fig. S1–S7†). After bromination and oxidative cyclization of **5**, the target monomer **7** was facilely obtained in four steps with the total yield around 25% (Scheme 1). From the key compound 7, both the small molecule (**TNTPT**) and the polymer (**PTNTPT-BDTT**) of the perylene-embedded benzothiazolyl can be prepared by the debromination reaction and the Stille coupling polycondensation, respectively.

Owing to the introduction of the long alkoxy groups on the benzothiazolyls, both **TNTPT** and **PTNTPT-BDTT** show excellent solubility in common solvents, which is favorable for the spin-coating processing of the active layers during OPV device fabrication. Meanwhile, the embedded rigid perylene enables their good thermal stabilities as revealed by thermal gravimetric analysis (TGA) measurements with the decomposition temperature (Td) over 300 °C at a 5% weight loss; the Td of **TNTPT** (310 °C) is about 45 °C higher than that of **DTBT** (265 °C),[14] leading to further improved stability (T_d = 350 °C) of its copolymer (**PTNTPT-BDTT**). The simultaneously achieved good solubility and stable thermal properties of the perylene-embedded benzothiazolyls (Table 1) are highly applausive for OPV materials to support the solution processing of the device and long-term stability upon exposure to the solar luminescence in the device operation.[15]

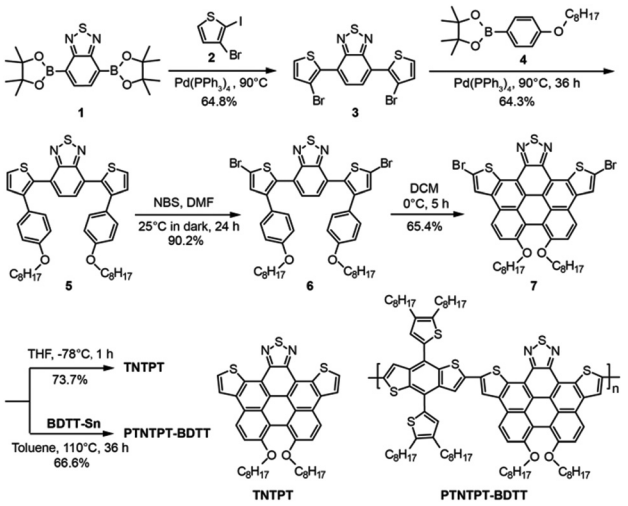

Scheme 1 Synthetic route to perylene-embedded benzothiazolyl (**TNTPT**) and its polymer (**PTNTPT-BDTT**).

To probe the validity of our design strategy for OPV donor materials, the frontier orbital energy levels of **TNTPT** and **PTNTPT-BDTT** were investigated using cyclic voltammetric (CV) measurements.[16] From the onset potential of the oxidation waves at 0.49 and 0.53 V, the HOMO energy levels of **TNTPT** and **PTNTPT-BDTT** were determined to be −5.28 and −5.32 eV, respectively (Fig. S8†). Combined with the optical energy bandgaps (E_g) of 1.94 and 1.60 eV measured by the absorption onsets at 638 and 770 nm in the solid film, their LUMO energy levels were identified to be −3.34 and −3.72 eV (Table 1). In comparison with the optimal HOMO and LUMO energy levels of −5.4 and −3.9 eV with an E_g of 1.5 eV of ideal OPV donor materials using the typical acceptor [6,6]-phenyl-C61-butyric acid methyl ester ($PC_{61}BM$),[17] the values of **PTNTPT-BDTT** are much better than those of the widely used P3HT (poly(3-hexylthiophene), HOMO = −5.15 eV; E_g = 1.9 eV)[18] and **PDTBT-BDTT** (scheme S1,† HOMO = −5.26 eV; E_g = 1.74 eV),[19] showing the great potential of this newly designed perylene-embedded benzothiazolyl as a promising electron-deficient building block for OPV applications.

Density functional theory (DFT) calculations were then carried out to figure out the tuning mechanism of the 2D-fusing molecular design strategy for OPV materials (Fig. 2). The initial **DTBT** has a low LUMO of −2.61 eV in theory and −3.40 eV in experiment with a small bandgap, showing clearly its electron accepting feature.[7] The fusing of the surrounding thiophene and the core benzothiadiazole using ethylene leads to an increased LUMO and a decreased HOMO with an enlarged E_g, which can be understood according to our previously proposed HOMO–LUMO interaction model established in the investigation of heterofluorenes.[20] To reduce E_g for absorbing maximum sunlight in OPV applications, conjugated biphenyl is fused to **DTBT** two-dimensionally to afford a perylene-embedded benzothiazolyl of **TNTPT**, which shows both higher LUMO and HOMO but smaller E_g than **DTBT** due to extended π-conjugation. In light of the low LUMO of **TNTPT** (−2.33 eV in theory and −3.34 eV in experiment), the widely used BDTT was adopted as a comonomer to construct a conjugated copolymer[21] following a "weak donor–strong acceptor" strategy reported previously in designing the **DTBT** and BDTT

Table 1 The physical, optical, and electrochemical properties of **DTBT**,[14] **TNTPT**, **PDTBT-BDTT**,[19] and **PTNTPT-BDTT**

Molecule	T_d (°C)	M_w (kDa)	M_n (kDa)	PDI	λ_{peak} (nm)		E_g^{opt} (eV)	CV (eV)		DFT[a] (eV)	
					THF	Film		HOMO	LUMO	HOMO	LUMO
DTBT	265	0.30	0.30	1.0	445	471	2.16	−5.56	−3.40	−5.35	−2.61
TNTPT	310	0.70	0.70	1.0	544	565	1.94	−5.28	−3.34	−4.79	−2.33
PDTBT-BDTT	—	59	24	2.5	560	600	1.74	−5.26	−3.10	−4.97	−2.68
PTNTPT-BDTT	350	73	53	1.4	655	658	1.60	−5.32	−3.72	−4.69	−2.40

[a] The DFT calculated HOMO and LUMO energy levels of the repeating unit of copolymers.

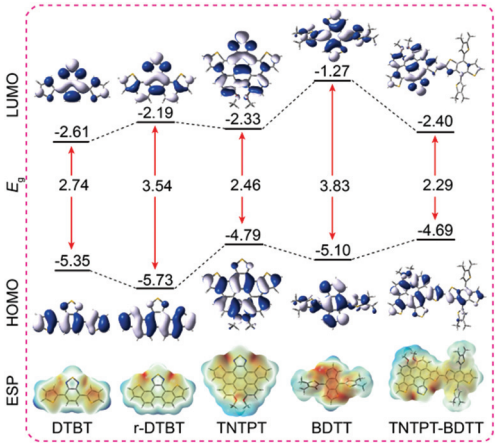

Fig. 2 DFT calculated HOMO, LUMO, bandgap (E_g), frontier orbital isosurface, and electrostatic potential (ESP) of **DTBT**, r-**DTBT**, **TNTPT**, **BDTT**, and **TNTPT-BDTT**.

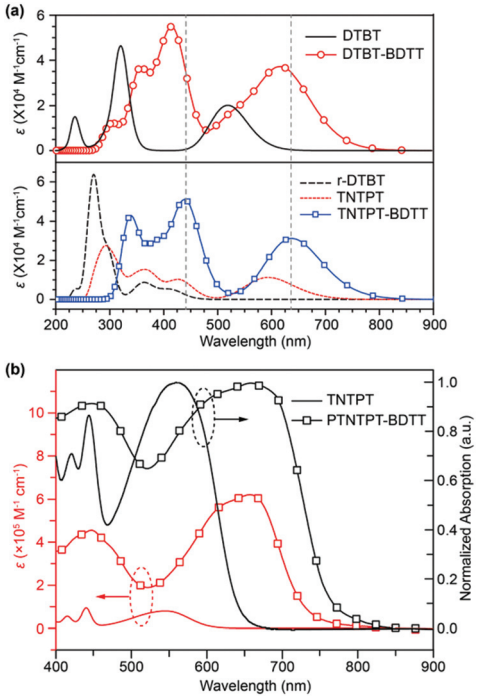

Fig. 3 (a) DFT simulated absorption spectra of **DTBT**, r-**DTBT**, **DTBT-BDTT**, **TNTPT**, and **TNTPT-BDTT**; (b) experimentally measured UV-Vis absorption spectra of **TNTPT** and **PTNTPT-BDTT** in films (black) and in solution with molar absorptivity (ε) (red).

copolymer of **PDTBT-BDTT**.[19] The dominated LUMO wave function distribution on the **TNTPT** unit of the repeating unit (**TNTPT-BDTT**) demonstrates clearly the acceptor feature of **TNTPT**; while the nearly equal contributions of the two monomers on HOMO suggest that BDTT indeed acts as a weak donor in the copolymer, leading to the highest HOMO and the lowest E_g of **TNTPT-BDTT**. Furthermore, the continuous and flat electrostatic potential (ESP) of **TNTPT-BDTT** in the donor–acceptor architecture is favorable for efficient charge transport after exciton dissociation during OSC operation. These theoretical insights suggest that 2D-fusing is highly effective in π-conjugation extending for decreased E_g with high π-electron delocalization for carrier migration.

Another important factor for an efficient OPV material is the high photo-absorption ability in a wide range of wavelengths that covers the whole sunlight spectrum. Therefore, the absorption spectra of **TNTPT** and **PTNTPT-BDTT** were experimentally measured to assess their sunlight absorption abilities and theoretically simulated to shed light on the structure–property relationship of the 2D-fused **DTBT**s. From DFT simulations (Fig. 3a), the fusing of **DTBT** (r-**DTBT**) with ethylene leads to enhanced and blue-shifted absorption, due to its rigid molecular structure, overlapped LUMO and HOMO distributions and enlarged E_g as the frontier orbital analysis indicates (Fig. 2). The 2D-fusing with biphenyl, however, results in a significantly red-shifted UV absorption spectrum, and it is further red-shifted (up to 50 nm) and enhanced (almost 2 fold) after the copolymerization with BDTT as in **TNTPT-BDTT**. In good accordance with the theoretical predictions, the experimentally measured UV-vis absorption spectra (Fig. 3b) of **TNTPT** are peaked at 548 and 550 nm in THF and film respectively, which are significantly red-shifted in comparison with that of **DTBT** at 445 and 471 nm; the copolymer of **PTNTPT-BDTT** exhibits broader and more red-shifted absorption spectrum with an onset absorption of 770 nm (1.60 eV), which is very close to the ideal optical bandgap of 1.50 eV for optimal sunlight absorption. The small red-shift (<5 nm) of the absorption peaks between that in solution and film is in line with the rigid molecular structure of the perylene-embedded benzothiazolyl monomer (**TNTPT**) and the polymer (**PTNTPT-BDTT**). Moreover, **TNTPT** has a very high molar extinction coefficient (ε = 9.5 × 10^4 M^{-1} cm^{-1}), while that of **PTNTPT-BDTT** (ε = 6.6 × 10^5 M^{-1} cm^{-1}) is even higher; these values are among the highest ε of OPV donors,[22] indicating the great potential of the new building block in sunlight absorption for OPV applications.

In light of the suitable frontier orbital energy levels for exciton dissociation and the optimal optical bandgap with a high molar extinction coefficient for sunlight absorption, the photovoltaic properties of **PTNTPT-BDTT** as an organic donor in BHJ solar cells were investigated. Devices A, B, and C were fabricated[23] in a conventional device structure of ITO/PEDOT:PSS (40 nm)/polymer : acceptor (120 nm)/Ca/Al (Fig. S9†). With the aid of the widely used acceptor of $PC_{61}BM$, the additive-free BHJ OSCs based on **PTNTPT-BDTT** show the highest PCE of 1.84% when the weight content of $PC_{61}BM$ is 50% (Table S1†). At this donor/acceptor weight ratio (1 : 1), the device performance was improved (PCE = 2.15%) using the additive 1-chloronaphthalene (CN), probably due to the formation of a better bi-phase interpenetrating network of the donor and acceptor with enhanced phase separation and increased sunlight absorption for a significantly increased short-circuit current density (J_{sc}) and decreased serial resist-

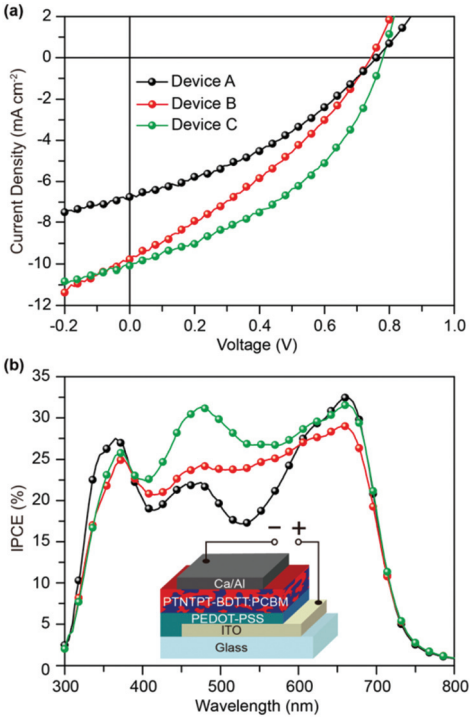

Fig. 4 (a) Current density–voltage (*J*–*V*) curves under AM 1.5G illumination (100 mW cm^{-2}) and (b) incident photon to current efficiency (IPCE) spectra of devices A–C. Inset, the BHJ OPV device structure.

ance (R_s). When a stronger sunlight absorber $PC_{71}BM$ is adopted as the acceptor, the device performances are further improved to PCE = 2.36% and 3.22% using additives 3 vol% diiodooctane (DIO) and CN, respectively (Fig. 4). To our delight, the preliminary performance of the new OPV material with a PCE up to 3.22% and an open circuit voltage (V_{oc}) around 0.75 V is better than that of **PDTBT-BDTT** in PCE (2.11%),[19] and comparable to that of the sophisticated devices of P3HT (PCE = 3.5%, V_{oc} = 0.60 V),[18] indicating the effectiveness of our design of the perylene-embedded benzothiazolyls *via* the 2D-fusing strategy for OPV applications (Table 2). The small fill factor (FF) may be due to the relatively poor morphology of the blend film (Fig. S10†), although a higher hole mobility (2.1×10^{-5} cm^2 V^{-1} s^{-1}) than that of **PDTBT-BDTT** (4.4×10^{-6} cm^2 V^{-1} s^{-1}) was identified (Fig. S11†).

In summary, we have synthesized a novel OPV building block of perylene-embedded benzothiazolyl (**TNTPT**) *via* a facile four-step synthetic route. This new OPV unit designed by 2D-fusing of **DTBT** shows a low optical bandgap with electron-accepting properties and high molecular rigidity with high thermal stability. When copolymerized with the electron-donating BDTT unit, the absorption profile of the copolymer (**PTNTPT-BDTT**) was red-shifted to a bandgap of 1.60 eV with strong sunlight absorption ability ($\varepsilon = 6.6 \times 10^5$ M^{-1} cm^{-1}), and the frontier orbital energy levels were fine-adjusted to −5.32 (HOMO) and −3.72 eV (LUMO), approaching the optimal values of ideal OPV materials. Preliminary solution-processed BHJ OSCs using $PC_{71}BM$ as the acceptor and aromatic CN as the additive gave a PCE of 3.22%, which is much higher than that of the non-fused **PDTBT-BDTT** in a similar device structure and comparable to that of the widely investigated P3HT-based OSCs. These findings are important not only for highlighting the feasibility of the 2D-fusing strategy on the widely-used electron-accepting **DTBT** to achieve low bandgap acceptors as new building blocks for OPV material design, but also for providing a convenient route for the facile synthesis of 2D-fused molecules containing both rigid perylenes and soluble substituents.

Table 2 Photovoltaic performance of **PTNTPT-BDTT**:PCBM (w/w, 1 : 1) BHJ devices

	Acceptor	Additive	J_{sc} (mA cm^{-2})	V_{oc} (V)	FF (%)	PCE (%)
A	$PC_{61}BM$	—	6.75	0.76	35.8	1.84
B	$PC_{71}BM$	DIO	9.78	0.74	32.7	2.36
C	$PC_{71}BM$	CN	10.07	0.78	41.1	3.22

This study was supported in part by the National Natural Science Foundation of China (21274065, 21304049, 61204048, 21574068, and 51173081), the Qing Lan project of Jiangsu province, and the Science Fund for Distinguished Young Scholars of Jiangsu Province of China (BK20150041).

Notes and references

1 K. A. Mazzio and C. K. Luscombe, *Chem. Soc. Rev.*, 2015, **44**, 78.
2 Z. He, B. Xiao, F. Liu, H. Wu, Y. Yang, S. Xiao, C. Wang, T. P. Russell and Y. Cao, *Nat. Photonics*, 2015, **9**, 174.
3 C. C. Chen, W. H. Chang, K. Yoshimura, K. Ohya, J. You, J. Gao, Z. Hong and Y. Yang, *Adv. Mater.*, 2014, **26**, 5670.
4 (*a*) G. Li, R. Zhu and Y. Yang, *Nat. Photonics*, 2012, **6**, 153; (*b*) L. YongFang, *Acc. Chem. Res.*, 2012, **45**, 10.
5 (*a*) H. Wang, Q. Shi, Y. Lin, H. Fan, P. Cheng, X. Zhan, Y. Li and D. Zhu, *Macromolecules*, 2011, **44**, 4213; (*b*) W. Zhou, F. Jin, X. Huang, X. M. Duan and X. Zhan, *Macromolecules*, 2012, **45**, 7823; (*c*) Y. Liu, H. Wang, H. Dong, J. Tan, W. Hu and X. Zhan, *Macromolecules*, 2012, **45**, 1296.
6 (*a*) M. E. Cinar and T. Ozturk, *Chem. Rev.*, 2015, **115**, 3036; (*b*) H. Zhou, L. Yang, S. Stoneking and W. You, *ACS Appl. Mater. Interfaces*, 2010, **2**, 1377.
7 B. Liu, A. Najari, C. Pan, M. Leclerc, D. Xiao and Y. Zou, *Macromol. Rapid Commun.*, 2010, **31**, 391.
8 (*a*) H. Zhou, L. Yang, S. C. Price, K. J. Knight and W. You, *Angew. Chem., Int. Ed.*, 2010, **49**, 7992; (*b*) H. Zhou, L. Yang, A. C. Stuart, S. C. Price, S. Liu and W. You, *Angew. Chem., Int. Ed.*, 2011, **50**, 2995; (*c*) R. Chen, Y. Wang, T. Chen, H. Li, C. Zheng, K. Yuan, Z. Wang, Y. Tao, C. Zheng and W. Huang, *J. Phys. Chem. B*, 2015, **119**, 583.
9 M. Bendikov, F. Wudl and D. F. Perepichka, *Chem. Rev.*, 2004, **104**, 4891.

10 Z. An, C. Zheng, Y. Tao, R. Chen, H. Shi, T. Chen, Z. Wang, H. Li, R. Deng, X. Liu and W. Huang, *Nat. Mater.*, 2015, **14**, 685.
11 Y. Zhang, Y. Xiao, Y. Xie, L. Zhu, D. Shi and C. Cheng, *Org. Electron.*, 2015, **21**, 184.
12 L. Huo, S. Zhang, X. Guo, F. Xu, Y. Li and J. Hou, *Angew. Chem., Int. Ed.*, 2011, **50**, 9697.
13 S. Gronowitz and B. Holm, *Acta Chem. Scand., Ser. B*, 1976, **30**, 423.
14 Z. Wang, Q. Liu, T. Chen, Y. Wang, J. Yuan, C. Zheng, R. Chen and W. Huang, *Dyes Pigm.*, 2015, **113**, 529.
15 M. Zhang, Y. Sun, X. Guo, C. Cui, Y. He and Y. Li, *Macromolecules*, 2011, **44**, 7625.
16 Y. Tao, J. Xiao, C. Zheng, Z. Zhang, M. Yan, R. Chen, X. Zhou, H. Li, Z. An, Z. Wang, H. Xu and W. Huang, *Angew. Chem., Int. Ed.*, 2013, **52**, 10491.
17 M. C. Scharber, D. Mühlbacher, M. Koppe, P. Denk, C. Waldauf, A. J. Heeger and C. J. Brabec, *Adv. Mater.*, 2006, **18**, 789.
18 M.-C. Wu, Y.-Y. Lin, S. Chen, H.-C. Liao, Y.-J. Wu, C.-W. Chen, Y.-F. Chen and W.-F. Su, *Chem. Phys. Lett.*, 2009, **468**, 64.
19 M. Wang, X. Hu, P. Liu, W. Li, X. Gong, F. Huang and Y. Cao, *J. Am. Chem. Soc.*, 2011, **133**, 9638.
20 R. F. Chen, C. Zheng, Q. L. Fan and W. Huang, *J. Comput. Chem.*, 2007, **28**, 2091.
21 (*a*) J. M. Jiang, H.-K. Lin, Y.-C. Lin, H.-C. Chen, S.-C. Lan, C. K. Chang and K. H. Wei, *Macromolecules*, 2014, **47**, 70; (*b*) J. M. Jiang, P. Raghunath, H. K. Lin, Y. C. Lin, M. C. Lin and K.-H. Wei, *Macromolecules*, 2014, **47**, 7070; (*c*) Y. W. Su, S. C. Lan and K. H. Wei, *Mater. Today*, 2012, **15**, 554.
22 F. Xu, L. Peng, K. Shinohara, T. Nishida, K. Wakamatsu, M. Uejima, T. Sato, K. Tanaka, N. Machida, H. Akashi, A. Orita and J. Otera, *Org. Lett.*, 2015, **17**, 3014.
23 P. Kumar, C. Bilen, K. Feron, N. C. Nicolaidis, B. B. Gong, X. Zhou, W. J. Belcher and P. C. Dastoor, *ACS Appl. Mater. Interfaces*, 2014, **6**, 5281.